Talanta 232 (2021) 122408

Contents lists available at ScienceDirect

Talanta

journal homepage: www.elsevier.com/locate/talanta

Sandpaper-based electrochemical devices assembled on a reusable 3D-printed holder to detect date rape drug in beverages

Danielly S. Rocha [a], Lucas C. Duarte [a], Habdias A. Silva-Neto [a], Cyro L.S. Chagas [b], Mário H. P. Santana [c], Nelson R. Antoniosi Filho [a], Wendell K.T. Coltro [a,d,*]

[a] Instituto de Química, Universidade Federal de Goiás, 74690-900, Goiânia, GO, Brazil
[b] Instituto de Química, Universidade de Brasília, 70910-900, Brasília, DF, Brazil
[c] Unidade Técnico-Científica – Superintendência Regional da Polícia Federal Em MG, Uberlândia, MG, 38408- 6630, Brazil
[d] Instituto Nacional de Ciência e Tecnologia de Bioanalítica, 13083-861, Campinas, SP, Brazil

ARTICLE INFO

Keywords:
Electrochemical sensors
Forensic chemistry
Paper-based sensors
Pulse voltammetry
3D printing

ABSTRACT

This study describes the development of a new electrochemical paper-based analytical device (ePAD) on alumina sandpaper substrate through a pencil-drawing process for square wave voltammetry measurements of midazolam maleate used as a "date rape drug" in beverages. The proposed ePAD was assembled on a reusable 3D printed holder to delimit its geometric area and ensure better robustness. The ePAD was characterized by scanning electron microscopy, cyclic voltammetry, electrochemical impedance spectroscopy and Raman spectroscopy. The direct drawing of ePADs on sandpaper platforms through a graphite pencil has offered suitable repeatability (RSD = 1.0%) and reproducibility (RSD = 4.0%) using $[Fe(CN)_6]^{4-}$ as redox probe. The proposed ePAD provided linear behaviour in the midazolam maleate concentration range between 2.5 and 150 mg L^{-1} and a limit of detection of 2.0 mg L^{-1}. The feasibility of the ePAD for forensic application was successfully demonstrated through the detection of midazolam in different beverages (water, beer, liquor, and vodka). The intended application revealed low interference of other compounds present in beverages. Based on the achieved results, the proposed ePAD has offered great accuracy with no statistical difference at 95% confidence level from the data recorded by high performance liquid chromatography. The operational simplicity and the robustness ensured by the assembling on a reusable 3D printed holder make the ePAD drawn on sandpaper platform a powerful and promising analytical tool for the analysis of "date rape drugs" opening new possibilities for on-site forensic investigations.

1. Introduction

Flunitrazepam, ketamine, gamma hydroxybutyric acid, and midazolam maleate are sedative drugs widely used in drug-facilitated crimes (DFCs) according to the United Nations Office on Drugs and Crime (UNODC) [1–5]. The combined intake of these sedatives in alcoholic beverages can cause severe central nervous system depression, leading to the depletion of cognitive function, memory loss, and, in more severe cases, the individual's death. As such, these drugs are usually added to drinks without the victim noticing, leading to loss of consciousness, amnesia, or hallucination. Thus, the victim may be vulnerable to various crimes, such as sexual crimes, theft, and the stealing of bank information [6–9]. Among these DFCs, midazolam maleate has emerged as one of the most used drugs due to its rapid action on the human body. This drug and its metabolites provide rapid delivery in the human organism, which can difficult the detection in biological matrices. In this sense, the direct analysis of this drug in alcoholic beverages can result in a promising tool for forensic studies [4,6,10,11].

The most common techniques for midazolam analysis are high-performance liquid chromatography (HPLC) [6,12], gas chromatography [11,13], spectrophotometry [14], and capillary zone electrophoresis coupled to mass spectrometry [15]. However, these methods need a large amount of reagents and samples, resent limited portability, require a longer training time for the analyst, and are costly due to their sophisticated instrumentation [10]. On the other hand, electrochemical methods are excellent alternatives because they are considered low cost and compatible with the miniaturization, thus requiring smaller sample volumes and providing potentially portable instrumentation, which is

* Corresponding author. Instituto de Química, Universidade Federal de Goiás, Campus Samambaia, 74690-900, Goiânia, GO, Brazil.
E-mail address: wendell@ufg.br (W.K.T. Coltro).

https://doi.org/10.1016/j.talanta.2021.122408
Received 13 January 2021; Received in revised form 4 April 2021; Accepted 7 April 2021
Available online 20 April 2021

interesting for on-site applications. Electrochemical methods are also advantageous when compared to conventional techniques often explored for midazolam analysis, such as selectivity due to oxidation and/or reduction specific potentials of electroactive species, suitable sensitivity when using pulsed voltammetric methods such as differential pulse voltammetry (DPV) and square wave voltammetry (SWV) [16,17], in addition to the possibility of reaching low detection limits by modifying the working electrode surface.

In this context, the development of miniaturized and simple-to-manufacture electrochemical paper-based analytical devices (ePADs) has grown in recent years since they can be made of affordable, alternative, and low-cost materials, presenting good analytical performance [17–20]. Several paper-based platforms have been used to fabricate electrochemical cells, including chromatographic paper [21], filter paper [22], sulphite paper [23], fiberboard [24], paperboard [25], vegetal paper [26], waterprooof paper [27], and sandpaper [28]. Although sandpaper is not yet a widely explored platform, it has some desirable features to fabricate ePADs, such as good mechanical strength, flexibility, abrasion, hydrophobicity, and the possibility of surface modification. Recently, Xu and colleagues published a study describing the development of an electrochemical sensor using the laser engraving technique on alumina sandpaper. In this device, the alumina sandpaper surface was modified with nickel, creating a reusable non-enzymatic sensor for glucose detection in human serum samples [29].

Typically, the manufacturing processes for ePADs reported in the literature include screen-printing [30,31], inkjet printing [32], laser scribing [25,33] stencil-printing [34], pencil drawing [4,35–38], or pen friction drawing [39] protocols. Among these processes, pencil drawing has received significant attention from the scientific community in recent years and is one of the simplest, fastest, and cheapest methodologies to create paper-based devices [19,36,40]. The pioneering study for the manufacturing of an ePAD via a pencil drawing protocol was reported by Dossi and co-workers, where the electrochemical cell was drawn directly on a strip of chromatographic paper and the wax printing process was used to define the area of a set of electrochemical cells. This sensor was used for the electrochemical separation and detection of ascorbic acid and sunset yellow dye [35].

Dias and colleagues recently reported the manufacture of an ePAD by a pencil drawing technique on vegetal paper, and a polyester lamination process was used to delimit the geometric area of the electrochemical cell. This ePAD was used for the detection of analgesic and sedative drugs, including midazolam, in whiskey samples of forensic interest [4].

3D printing is another emerging technology for the development of analytical devices [41] including for example, electrochemical sensors [42], wearable sensors [43], microfluidic devices with integrated sensing electrodes [44], holders coupled to a smartphone [45], high-relief masters for replicating poly(dimethyl)siloxane (PDMS) microchannels [46], among others. Recently, Scordo and co-workers developed a 3D-printed holder as a sample reservoir incorporated into an ePAD modified with carbon black and a Prussian blue nanocomposite to measure the activity of the enzyme butyrylcholinesterase in human serum samples [41].

In this sense, we describe the development of an ePAD using the direct graphite pencil drawing process on an alumina polishing sandpaper platform. In addition, the ePAD was coupled for the first time onto a reusable 3D-printed holder for multiple purposes, such as electrical contact isolation and geometric area delimitation aiming to decrease the sample evaporation rate. As a proof of concept, the proposed ePAD assembled on a 3D-printed holder was explored for the detection of midazolam maleate in different matrices commonly used for "date rape drug" crimes, such as water, beer, liquor, and vodka.

2. Materials and methods

2.1. Chemicals and materials

Potassium ferrocyanide, potassium ferricyanide, potassium chloride, sodium dihydrogen phosphate, sodium hydrogen phosphate, sodium citrate, polyethylene glycol (PEG 6000), lactose, citric acid, ammonium chloride, methanol, and acetonitrile were purchased from Sigma-Aldrich (St. Louis, MO, USA). Sylgard 184 elastomer kit (monomer and curing agent) was acquired from Dow Corning (Midland, MI, USA). Midazolam maleate was donated by Polícia Federal (Uberlândia, MG, Brazil). Stock and standard solutions were prepared using ultrapure water processed through a water purification system (Direct-Q® 3, Millipore, Darmstadt, Germany) with resistivity equal to 18.2 MΩ cm.

The 1000-mesh polishing sandpaper, model A275, was purchased from Norton/Saint-Gobain (Worcester, MA, USA). 6B aquarelle pencil graphite was acquired from KOH-I-NOOR (Budweis, Czech Republic). Silver ink (Model 6130 M, lot number 150902) was obtained from Method Development Co. (Chicago, IL, USA). The acrylonitrile butadiene styrene (ABS) and flexible polylactic acid (PLA-Flex) thermoplastic filaments (ø = 1.75 mm), supplied by 3D Fila (Belo Horizonte, MG, Brazil), were used to manufacture the 3D-printed holder.

2.2. Fabrication of ePAD and 3D-printed holder

The electrodes were fabricated using the graphite pencil by direct friction on sandpaper surface. Fig. 1 summarizes the ePAD manufacturing steps and the coupling with the 3D-printed holder. First, the electrode array layout was drawn in graphical software (CorelDraw Graphics Suite X7™) and contained a working electrode (ø = 4 mm), a counter electrode, and a reference electrode. The ePAD design (lines) was printed on 1000-mesh polishing sandpaper by using an inkjet printing. The counter and working electrodes were painted with a water-based graphite pencil (Fig. 1A). Then, the pseudo reference electrode was painted with silver ink (Fig. 1B).

To delimit the geometric area, an ePAD holder was manufactured via 3D printing. The 3D-printed holder was designed using the graphical software AutoCAD® 2016 (Autodesk Inc., San Rafael, CA, USA) and printed by an Original Prusa i3 mk2/S 3D printer (Prusa Research, Prague, Czech Republic). The printing process was performed for about

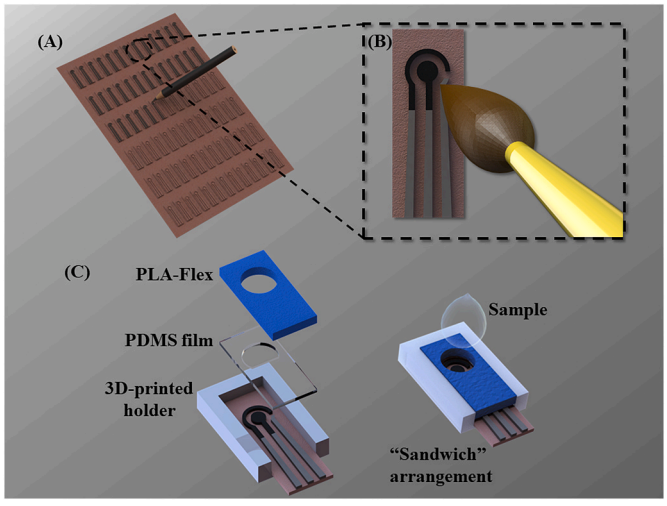

Fig. 1. Schematic representation of the sandpaper electrodes manufacturing process and 3D-printed holder. (A) Layouts of the electrodes under preparation on sandpaper substrate by pencil drawing. (B) Electrical contacts and the reference electrode painted with silver ink. (C) Components of the "sandwich" arrangement between the 3D-printed holder, PDMS film, electrode and top cover with PLA-Flex.

40 min using ABS and PLA-Flex thermoplastic filaments. The integration between the ePAD and the 3D-printed holder was accomplished by inserting the electrode into the 3D-printed holder. A PDMS film (thickness *ca.* 2 mm) was placed over the electrode to prevent any solution leakage. The PLA-Flex cover was attached to keep the system fixed, thus forming a "sandwich" arrangement between the holder base, ePAD, PDMS, and PLA-Flex, as shown in Fig. 1C. For a better visualization, a real image showing the assembling of electrochemical device inside the 3D-printed holder is demonstrated in Fig. S1.

2.3. Midazolam maleate analysis

The procedure for midazolam maleate analysis was adapted from the protocol reported by Dias et al. [4]. For the SWV measurements, the stock solutions of the midazolam maleate were prepared in water, beer, liquor and vodka containing 0.1 mol L^{-1} KCl and 0.1 mol L^{-1} phosphate buffer (pH 3.5). For the SWV analysis in water, the proportion of water: KCl:phosphate buffer (pH 3.5) was 8:1:1. For alcoholic beverage analyzes, the proportion adopted for target drink:KCl:phosphate buffer (pH 3.5) was 7:2:1. Considering the drink sample preparation, the final concentrations of alcohol was ~16.8% (beer), 3.25% (liquor) and 28% (vodka). The SWV parameters were the following: potential range of −0.25 to −1.2 V, amplitude of 0.004 V, step of 0.002 V, and frequency of 1 Hz. All electrochemical measurements were recorded at room temperature (25 ± 2) °C.

The reference analysis of midazolam maleate in alcoholic beverage samples was performed by HPLC according to the protocol adapted from Laviana et al. [12]. The experiments were carried out using a liquid chromatograph model 12200 Infinity LC (Agilent Technologies, Santa Clara, CA, USA) controlled by OpenLAB CDS software and equipped with a reverse phase chromatographic column (C18, 150 mm × 2.1 mm, 2.7 μm) at 30 °C. The mobile phase used was ammonium chloride/methanol/acetonitrile (45:22:33, v/v/v) with a flow rate of 1.2 mL min^{-1} and an injection volume of 10 μL. The diode array detector (DAD), model G4294B, was operated at a wavelength of 220 nm.

2.4. Electrical resistance, morphological, structural and electrochemical characterization

The electrical resistance of the conductive graphite trails made with the pencil on the sandpaper was measured using a multimeter (model 8846A) purchased from Fluke (Everett, WA, USA). Scanning electron microscopy (SEM) was used for surface morphological characterization of the ePAD using a JEOL microscope (model JSM, 6610, Waltham, MA, USA). Raman spectroscopy analysis was performed in a confocal Raman spectrometer (model Horiba LabRAM HR Evolution, HORIBA France SAS) using a laser of wavelength 532 nm and a spot size of 2.6 μm.

Cyclic voltammetry (CV) measurements were performed using 60 μL of 5 mmol L^{-1} $[Fe(CN)_6]^{4-}$ in 0.5 mol L^{-1} KCl and a bipotentiostat/galvanostat, model μStat 400 (DropSens S.L., Oviedo, Spain), equipped with DropView 2.9 software. The study of scanning rate was realized ranging from 20 to 100 mV s^{-1}. The comparison of electrochemical response between sandpaper ePAD and screen-printed carbon electrode (SPCE) model DS 110 (DropSens S.L., Oviedo, Spain) was also realized.

Electrochemical impedance spectrometry (EIS) measurements were carried out using the $[Fe(CN)_6]^{4-/3-}$ redox probe and a PGSTAT-100 potentiostat (Metrohm-Autolab, Netherlands) equipped with NOVA 2.1 software. The open-circuit potentials for experiments using the SPCE and the ePAD were 0.14 V and 0.18 V, respectively. The amplitude was 0.02 V and the frequency range was 10^5 to 10^{-1} Hz.

3. Results and discussion

3.1. Optimization of ePAD manufacturing

The first step in the fabrication of ePADs was the selection of the type of sandpaper and pencil, which were chosen based on the lowest electrical resistivity value measured for the paper and pencil assembly. For this purpose, trails of 1.5 cm × 0.1 cm were created by a pencil drawing protocol, and the electrical resistance values were measured with a digital multimeter. Sandpapers were evaluated with different grit size numbers (#1000 and #1200) and seven pencils with different degrees of hardness. The resistivity values obtained are shown in Table S1 (available in the electronic supplementary material, ESM).

Based on resistivity data, the sandpaper and pencil selected were Norton #1000 and KOH-I-NOOR Aquarelle 6B, respectively. The electrical resistivity value obtained was 61 ± 2 Ω cm (as shown in Table S1) and was comparable with the electrical resistivity value estimated by Santhiago and co-workers (157.5 Ω cm) using an electrode manufactured on office paper and graphite pencil 4B [38]. Recently, Dias et al. reported the fabrication of an ePAD using pencil (Aquarelle 6B) on vegetal paper, with an electrical resistivity values of 580 Ω cm [4], which is almost 10 times higher when compared to the current study. These results suggest that the sandpaper graphite electrode has low electrical resistivity. The lower electrical resistivity of this new ePAD may be related to the abrasive property of the sandpaper platform. This feature enables efficient graphite deposition on the paper surface, promoting suitable interconnectivity between graphite layer and substrate. Figure S2 exhibits a SEM image of the carbon film deposited on sandpaper platform through pencil drawing. The thickness value of conductive layer was estimated to be ca. 23 ± 3 μm. In addition, it was observed that the graphite microstructure was deposited uniformly along the conductive tracks as indicated by the appreciate resistivity of the proposed carbon-based material.

Some advantages of using sandpaper as a paper platform for the manufacture of electrodes are its easy access, low cost, durability, hydrophobicity, flexibility, appreciable mechanical resistance, and absence of capillary action, facilitating the isolation of the electrical contact. Furthermore, the time required for the fabrication of a single ePAD was approximately 15 min, including geometry printing, drawing with graphite pencils, painting with silver ink, and thickness adjustment with double-sided tape. Each piece of sandpaper (A4 size) can be used to print 100 electrodes, and the price per device was estimated to be *ca.* US $ 0.03.

3.2. 3D-printed holder

The 3D-printed holder arrangement had the function of delimiting the geometric area of the ePAD, promoting isolation of the electric contact, and acting as a reservoir for the sample, as shown in Fig. 1C and Fig. S1. The holder was printed using affordable, durable, and reusable 3D-printing features. In the proposed arrangement, the hydrophobic barrier is based on the application of force on the PLA-Flex cover, promoting PDMS compression. In addition, the electrochemical device can be easily exchanged by decompressing the PDMS film. Thus, once the hydrophobic barrier is reusable, one step in the ePAD manufacturing process was reduced compared to some reported protocols. The cost of the 3D-printed holder and PDMS film were *c.a.* US$ 0.04 and US$ 0.39, respectively. This value presented an excellent cost benefit as both the 3D device and PDMS film can be reused after simple cleaning with water (considering the use of aqueous solutions). The main disadvantages of the 3D-printed holder include its low resistance to organic solvents, thus making analysis in a non-aqueous medium difficult, and the need for an ePAD made of a hydrophobic material, as the PDMS film is not able to prevent the solution from flowing through the substrate. However, for electrochemical analysis in aqueous medium, the 3D printed piece has been a great holder to assemble the ePAD.

Scordo et al. developed a 3D-printed holder based in an open/close arrangement to provide robustness to the filter paper ePAD and to act as a reservoir. In their methodology, isolation of the electric contact was done by depositing hydrophobic barriers using wax heating [41]. Other works have employed the use of wax to create hydrophobic barriers [22,

35]. In other methodologies for the electrode manufacturing, the isolation of the electrical contact, as well as the delimitation of the geometric area of the electrode was carried out by means of irreversible processes such as the use of nail polish [47], electrical tape [48,49], thermal lamination [4,26], glue [25] or paraffin wax [50]. Thus, the hydrophobic insulator cannot be reused, therefore requiring an additional step in the manufacture of each electrochemical device.

3.3. Morphological characterization

The morphology of the sandpaper and the ePAD was evaluated by SEM (Fig. 2). As can be seen in Fig. 2A and B, the sandpaper has a rough and grooved surface composed of a set of small interlaced layers, characteristic of abrasive surfaces. Whereas after drawing the electrodes with a pencil (Fig. 2C), it was noted that a layer of graphite was deposited evenly on the sandpaper surface, leaving it smooth. This smoother profile indicates efficient deposition and good interconnectivity of the graphite layers during the friction process. In the working electrode of the ePAD, after 50 CV measurements, the surface morphology underwent some changes and became slightly worn and rough (Fig. 2D). Considering that the pencil used in the manufacture of the electrodes is water-soluble, it was expected that in the presence of an aqueous solution part of the deposited graphite would be leached, wearing the ePAD surface, making the proposed electrochemical sensor a disposable device.

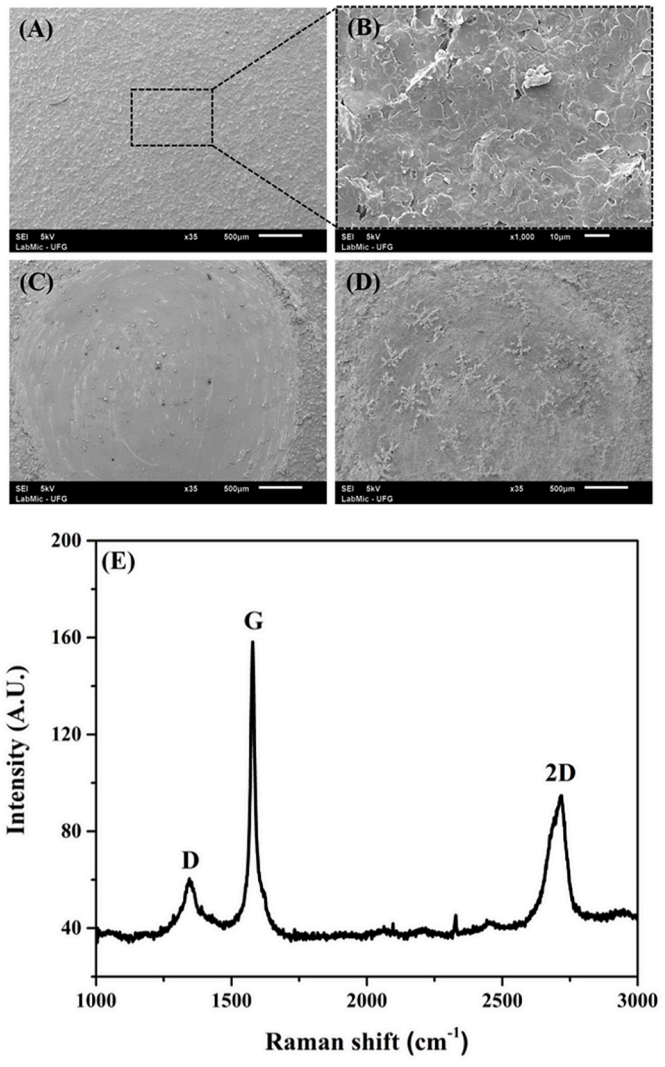

Fig. 2. SEM images of the sandpaper with (A) 35 magnification and (B) 1000 magnification. (C) Working electrode before use and (D) after 50 scans using 5 mmol L^{-1} $[Fe(CN)_6]^{4-}$ in 0.5 mol L^{-1} KCl at 20 mV s^{-1}. (E) Raman spectra ranging from 1000 to 3500 cm^{-1}.

Raman spectroscopy was explored to investigate the microstructures of the carbon-based surface. As displayed in Fig. 2E, the Raman spectra was recorded between 1000 and 3000 cm^{-1} and revealed bands D, G and 2D at 1344, 1574 and 2706 cm^{-1}, respectively. Based on achieved values, the I_D/I_G ratio was estimated to be 0.18. The obtained results have been reported as indicative to graphite-based microstructures [51] and they suggest that the proposed surface offer considerable structural defect when compared to pure graphite (0.014) [51,52]. The noticeable alteration in the structural defects of the proposed material may be associated to the presence of other components in the commercial graphite pencil, such as structural ceramics.

3.4. Electrochemical characterization

The electroanalytical feasibility of the proposed ePAD was evaluated by CV measurements, as displayed in Fig. S3 (available in the ESM). For this study, a 0.5 mol L^{-1} KCl (pH 7) electrolyte was used with a scan rate of 20 mV s^{-1} and a potential range of −1.5 to 1.5 V (Fig. S3-A). The voltammogram recorded exhibited a wide potential window (−1.3 to 1.3 V) and absence of redox species contamination from graphite pencil.

The effect of the scan rate between 20 and 100 mV s^{-1} on the electrochemical response was investigated using $[Fe(CN)_6]^{4-}$ in the CV measurements (Figs. S3-B and S3-C). Fig. S3-C shows that the anodic (i_{ap}) and cathodic (i_{cp}) peak current signals have a linear behaviour as a function of the square root of the scan rate, with correlation coefficients of 0.990 and 0.994, respectively. These results suggest that the process of mass transfer of the electroactive species at the electrolyte/ePAD interface is controlled by diffusion. In addition, the performance of ePADs has indicated that the larger sandpaper roughness can be incorporating effectively more graphite flakes, thus promoting an increase on the conductive contact surface when compared to other types of cellulose-based substrates.

The sandpaper electrode was compared to a commercial screen-printed carbon electrode (SPCE) supplied by DropSens (model DS 110). The parameters evaluated were the separation between the anodic and cathodic peak potentials (ΔEp) and the ratio between the anodic and cathodic peak currents, considering to scan at 20 mV s^{-1}. The ΔEp values were 190 and 156 mV and the ratio between i_{ap} and i_{cp} obtained were 0.96 and 1.01 for ePAD and SPCE, respectively. These values are associated with quasi-reversible processes. In reversible processes involving one electron, the separation between the peak potentials is approximately 59 mV [53]. The higher value for the peak separation when compared to the commercial SPCE may be associated to the greater electrical resistance of the electrode manufactured on sandpaper substrate. This behaviour can be related to the composition of the commercial pencil, which is not exclusively based on graphite structures, having in their formulation non-conductive materials such as ceramic materials [35,40]. The presence of non-conductive materials incorporated on the electrode surface can repel the redox mediator due to electrostatic repulsions. The values obtained for peak separation are relatively similar to those found in other studies reported in the literature. In previous studies reported independently by Dossi et al. [35] and Dias et al. [4], the ΔEp values for pencil-drawn electrodes in paper were 240 mV and 250 mV, respectively. However, the obtained values are slightly lower than the values reported in the aforementioned studies, thus demonstrating suitable feasibility for electrochemical purposes.

The ePAD and commercial SPCE were also characterized by the EIS technique using 5 mmol L^{-1} $[Fe(CN)_6]^{4-/3-}$ in 0.5 mol L^{-1} KCl. The semicircle of the Nyquist plot represents the electron-transfer resistance (R_{ct}), as denoted in Fig. S3-D. The charge-transfer resistance of the ePAD was 225 ± 4 Ω, while the commercial electrode has a charge-transfer resistance of 558 ± 2 Ω. Reis and co-workers compared the performance of electrodes manufactured by a laser-scribing process with the

conventional glassy carbon electrode and SPCE using EIS. The charge transfer resistance values were 80 ± 10, 240, and 360 Ω, respectively [25]. In addition, a recent study reported by Dias et al. showed values of 508 Ω and 490 Ω for flexible graphite electrodes and SPCE, respectively [52]. Therefore, the sandpaper ePAD presented a R_{ct} lower than these reported studies, which demonstrates the high efficiency of electron transfer in the newly developed ePAD. This agrees with the cyclic voltammograms displayed in Fig. S3-E. The voltammograms reveal that the i_{ap} and i_{cp} values for the ePAD are greater than those for the SPCE, as also indicated by the impedance, since the charge transfer resistance of this electrochemical mediator to the ePAD was lower than the commercial electrode.

To evaluate the mechanical resistance of the ePAD, CV was performed using 5 mmol L^{-1} $[Fe(CN)_6]^{4-/3-}$ as a redox probe in 0.5 mol L^{-1} KCl, with a scan rate of 50 mV s^{-1} and a potential window from −0.4 V to 0.8 V. Initially, CV was performed on the ePAD without bending it. Posteriorly, the sandpaper ePAD was bent up and down (90°; Fig. S4, available in the ESM) and additional CV measurements were performed (Fig. S3-F). This procedure was repeated 12 times. According to the results of the mechanical stress test, it was found that the values of i_{ap}, before and after bending, did not differ statistically at a confidence level of 95%. Thus, it can be said that the ePAD proposed in this study is versatile, since it has enough flexibility to be bent without loss in its analytical performance.

3.5. Repeatability, reproducibility, and durability

The repeatability and reproducibility of the ePAD were also evaluated through 10 CV measurements using 5 mol L^{-1} $[Fe(CN)_6]^{4-}$ in 0.5 mol L^{-1} KCl (Fig. 3A and B). The i_{ap} difference between measurements were 1% and 4% for repeatability and reproducibility, respectively. In other studies, Orzari and co-workers reported repeatability and reproducibility values for pencil-drawn electrodes on a fiberboard substrate of 3.2% and 4.0%, respectively [24], while Dossi and co-workers fabricated a polyvinyl chloride(PVC)-based pencil-drawn electrode, and the values obtained for repeatability and reproducibility studies were 3.8% and 5.6%, respectively [54]. Therefore, the values obtained here demonstrate excellent repeatability and reproducibility.

The durability was also evaluated through 50 CV measurements on the same ePAD, as can be seen in Fig. 3C. The sandpaper ePAD demonstrated good stability and durability (RSD = 3%), without a resistive profile, similar to the study reported by Pradella-Filho and co-workers, that also demonstrated high stability of paper-based electrodes following 100 successive CV measurements [47].

3.6. Analytical performance

The analytical performance of the sandpaper ePAD was evaluated in terms of midazolam maleate detection by SWV. The linear concentration ranged from 2.5 to 150 mg L^{-1} using a linear baseline correction for the recorded voltammogram (Fig. 4A). The analytical curve to midazolam maleate, and the linear equation obtained was i (μA) = −0.356 – 0.021 [midazolam maleate, mg L^{-1}], with R^2 = 0.998 (Fig. 4B). The limit of detection (LOD) was calculated based on 3σ of the background noise, and the value obtained was 2.0 mg L^{-1} (4.45 × 10^{-6} mol L^{-1} midazolam). The achieved LOD is enough to allow the detection of a fraction equivalent to 1/10 of a midazolam tablet per litre of beverage. The achieved detectability levels are considered suitable for forensic situations. O'Boyle et al. reported that dosages of midazolam ranging from 10 to 15 mg are capable to promote real effects in adult patients involving licit medicinal operations [55].

Table S2 (available in the ESM) summarizes different electrochemical sensors and the main electrochemical methods for the detection of midazolam. Considering the mentioned electrodes, electrochemical sensor based on mercury materials exhibits excellent surface renovation and faster electron transfer, however these electrodes are considered as non-environmentally friendly strategy. On other hand, the proposed ePAD is an alternative environmentally friendly and demonstrates adequate analytical performance when associated to pulse voltammetry based on SWV responses. As displayed in Table S2, different electrochemical techniques including potentiometry, differential pulse polarography (DPP), cyclic voltammetry (CV), square-wave cathodic stripping voltammetry (SWCSV) and SWV have been reported for analysing midazolam [4,7,10,56–59]. Among all of them, SWV is particularly advantageous when compared to potentiometry and CV techniques because it provides fast response and the best detectability levels. In addition, the explored electrochemical approach offering more quantitative information to the target redox species. Regarding to SWCSV method, this electrochemical approach offers pre-concentration step to increases the target signal responses. However, this important operation step can be considerable raises the analysis time.

3.7. Selectivity study and reusable 3D-printed holder

Possible interferences of midazolam maleate present in beverages or tablets were evaluated at a ratio of 5:1 (interfering:midazolam maleate) based on the current values in percentage of variation, as can be seen in Fig. S5-A (available in the ESM). The obtained values indicated a loss of signal in the presence of lactose and citric acid −5.3 and −9.6%, respectively. While, the interfering agents PEG 6000 and citrate exhibits signal increase ranging from 3.5 to 7.0%. These values are within an acceptable range for the detection of midazolam maleate.

The reuse of the 3D-printed holder and the inter-day reproducibility were evaluated for 7 days with measurements in triplicate per day (Fig. S5-B). The RSD was 3.2%, demonstrating considerable stability based on the electrochemical response of midazolam maleate recorded in different days. Moreover, the 3D-printed holder and PDMS film can be used multiple times. This reuse is based on electrode removal by

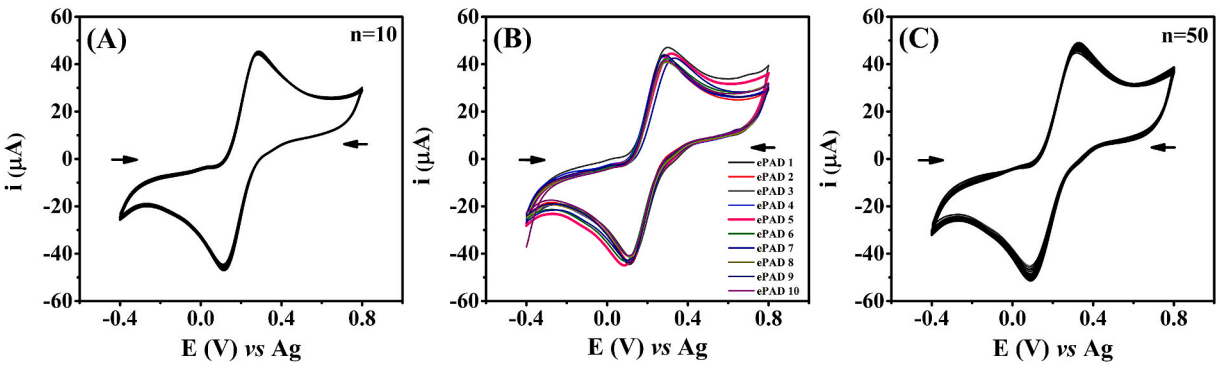

Fig. 3. Cyclic voltammograms for a redox probe composed of $[Fe(CN)_6]^{4-}$ (5 mmol L^{-1}) in 0.5 mol L^{-1} KCl recorded at 20 mV s^{-1} scan rate to investigate (A) repeatability, (B) reproducibility and (C) durability of the proposed electrochemical devices.

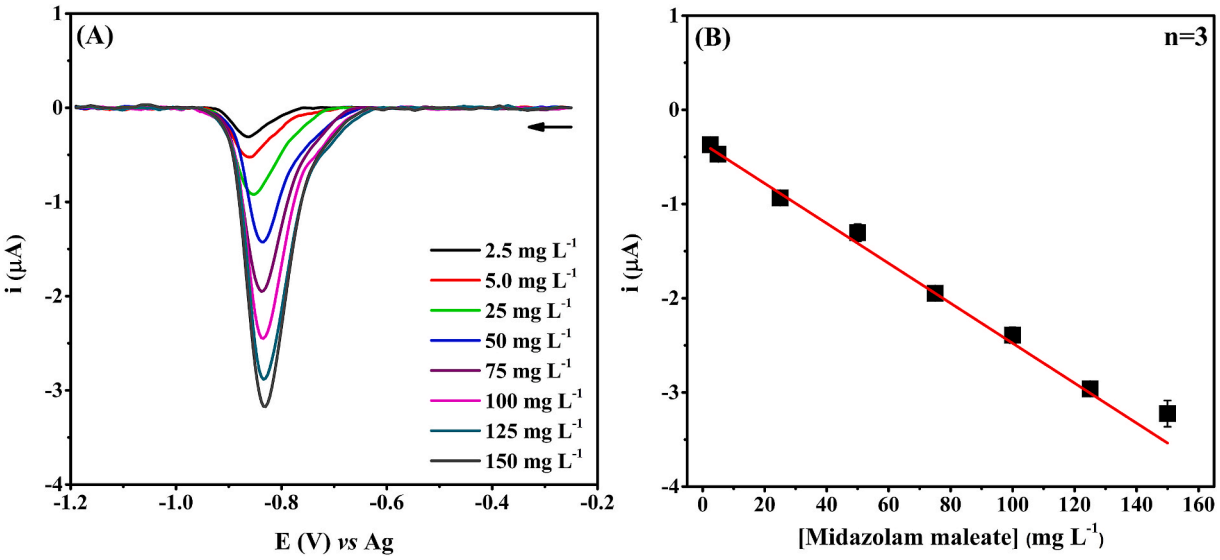

Fig. 4. (A) Square wave voltammograms obtained for midazolam maleate at different concentrations and (B) analytical curve.

decompression of the sandwich arrangement, replacement of the ePAD, and a new force application, interspersed with water wiping and drying of the device with a paper towel. It is noteworthy that all experiments were performed with the same support and the same PDMS film, which indicates a long service-life for 3D support and hydrophobic barriers.

3.8. Midazolam detection in beverage samples

The feasibility of the sandpaper ePAD was evaluated in different matrices of beverages that could be adulterated with midazolam maleate. Samples of water, beer, liquor, and vodka were spiked with 5 mg L^{-1} midazolam maleate and then analyzed by the conventional HPLC method and by SWV. The data recorded using both techniques are presented in Table 1. The square wave voltammograms and analytical curves used to quantify midazolam maleate in alcoholic beverages can be seen in Fig. S6-A-F. Moreover, a summary of the analytical data obtained for all matrices is displayed in.Table S3.

As can be noted in Table 1, the data obtained using SWV are in good agreement with those achieved through HPLC. A statistical paired *t*-test was applied using the determined analyte concentration. The calculated t values ranged between −1.88 and 0.89. Since they are lower than the t critical value (2.91), it can be inferred that there is no statistically significant difference at 95% confidence level between the two techniques. In this way, SWV has demonstrated be a reliable technique for the analysis of midazolam maleate in beverages. The operational simplicity, the low instrumental requirements and the possibility to allow on-site applications are attractive features for forensic purposes.

Table 1
Comparison of the midazolam maleate analysis in beverages using HPLC and SWV.

Beverages	HPLC (mg L^{-1})	SWV (mg L^{-1})
Water	4.61 ± 0.04	4.5 ± 0.6
Beer	4.80 ± 0.09	4.6 ± 0.7
Liquour	4.71 ± 0.04	4.5 ± 0.9
Vodka	4.17 ± 0.01	4.6 ± 0.3

4. Conclusions

In summary, an electrochemical sandpaper-based analytical device was developed for the first time by a pencil-drawing process, and for delimitation of the geometric area a reusable 3D-printed holder of "sandwich" arrangement with a hydrophobic barrier was proposed. This innovative system was applied for midazolam maleate detection in different beverages (water, beer, liquor, and vodka). The electrochemical cell combined with the 3D-printed holder showed a good mechanical resistance, repeatability, reproducibility, and durability. In addition, during the proof of concept, this method presented a good linear concentration range (2.5–150 mg L^{-1}), an LOD of 2.0 mg L^{-1}, selectivity for possible interferences, and accuracy, compared to the reference method (HPLC). The study of the 3D-printed holder as a reusable device was satisfactory (RSD < 3.16%). This robust ePAD assembled on a novel and reusable 3D-printed holder, has successfully demonstrated the detection of the presence of midazolam maleate in different drinks, thus being a powerful tool for the elucidation of "date rape drug" crimes.

Declaration of competing interest

The authors declare that they have no known competing financial interests or personal relationships that could have appeared to influence the work reported in this paper.

Acknowledgments

The authors would like to thank CAPES (grant 3363/2014), CNPq (grants 426496/2018-3, 308140/2016-8 and 307554/2020-1) and INCTBio (grant 465389/2014-7) for the financial support and granted scholarships. The authors acknowledge the Multi-user Laboratory of high-resolution microscopy (LabMic/UFG) for using their facilities during SEM and Raman measurements. Lastly, Dr. J. Pereira, A.A. Dias and Professor L.F. Sgobbi are also recognized for their technical support and helpful suggestions for this study.

Appendix A. Supplementary data

Supplementary data to this article can be found online at https://doi.org/10.1016/j.talanta.2021.122408.

Credit author statement

Danielly S. Rocha: Conceptualization; Data curation; Formal analysis; Investigation; Methodology; Software; Validation; Visualization; Writing - original draft. Lucas C. Duarte: Investigation; Methodology; Writing - review & editing. Habdias A. Silva-Neto: Investigation;

Methodology; Validation; Writing - review & editing. Cyro L. S. Chagas: Validation; Writing - review & editing. Mário H. P. Santana: Resources. Nelson R. Antoniosi Filho: Resources; Validation. Wendell K. T. Coltro: Resources; Funding acquisition; Project administration; Supervision; Writing - review & editing.

References

[1] F. Tseliou, P. Pappas, K. Spyrou, J. Hrbac, M.I. Prodromidis, Lab-on-a-screen-printed electrochemical cell for drop-volume voltammetric screening of flunitrazepam in untreated, undiluted alcoholic and soft drinks, Biosens. Bioelectron. 132 (2019) 136–142, https://doi.org/10.1016/j.bios.2019.03.001.

[2] A.M. Yehia, M.A. Farag, M.A. Tantawy, A novel trimodal system on a paper-based microfluidic device for on-site detection of the date rape drug "ketamine, Anal. Chim. Acta 1104 (2020) 95–104, https://doi.org/10.1016/j.aca.2020.01.002.

[3] R. Jiménez-pérez, J.M. Sevilla, T. Pineda, M. Blázquez, J. Gonzalez-rodriguez, Study of the electro-oxidation of a recreational drug GHB (gamma hydroxybutyric acid) on a platinum catalyst-type electrode through chronoamperometry and spectro-electrochemistry, J. Electroanal. Chem. 766 (2016) 141–146, https://doi.org/10.1016/j.jelechem.2016.02.005.

[4] A.A. Dias, T.M.G. Cardoso, C.L.S. Chagas, V.X.G. Oliveira, R.A.A. Munoz, C. S. Henry, M.H.P. Santana, T.R.L.C. Paixão, W.K.T. Coltro, Detection of analgesics and sedation drugs in whiskey using electrochemical paper-based analytical devices, Electroanalysis 30 (2018) 2250–2257, https://doi.org/10.1002/elan.201800308.

[5] A. Grela, L. Gautam, M.D. Cole, A multifactorial critical appraisal of substances found in drug facilitated sexual assault cases, Forensic Sci. Int. 292 (2018) 50–60, https://doi.org/10.1016/j.forsciint.2018.08.034.

[6] B. Daraei, K. Soltaninejad, M. Karimi, A. Nateghi, Simultaneous determination of six benzodiazepines in spiked soft drinks by high performance liquid chromatography with ultra violet detection (HPLC-UV), Iran, J. Pharm. Res. 15 (2016) 457–463, https://doi.org/10.22037/IJPR.2016.1863.

[7] N. Aliakbarinodehi, F. Stradolini, S.A. Nakhjavani, I. Tzouvadaki, I. Taurino, G. De Micheli, S. Carrara, Performance of carbon nano-scale allotropes in detecting midazolam and paracetamol in undiluted human serum, IEEE Sensor. J. 18 (2018) 5073–5081, https://doi.org/10.1109/JSEN.2018.2828416.

[8] R. Jain, R.K. Yadav, Voltammetric behavior of sedative drug midazolam at glassy carbon electrode in solubilized systems, J. Pharm. Anal. 2 (2012) 123–129, https://doi.org/10.1016/j.jpha.2011.11.08.

[9] F.P. Busardò, M.R. Varì, A.D.I. Trana, S. Malaca, J. Carlier, N.M. Di Luca, Drug-facilitated sexual assaults (DFSA): a serious underestimated issue, Eur. Rev. Med. Pharmacol. Sci. 23 (2019) 10577–10587, https://doi.org/10.26355/eurrev_201912_19753.

[10] Y. Panahi, A. Motaharian, M.R.M. Hosseini, O. Mehrpour, High sensitive and selective nano-molecularly imprinted polymer based electrochemical sensor for midazolam drug detection in pharmaceutical formulation and human urine samples, Sensor. Actuator. B Chem. 273 (2018) 1579–1586, https://doi.org/10.1016/j.snb.2018.07.069.

[11] J. Vasiliades, T. Sahawneh, Midazolam determination by gas chromatography, liquid chromatography and gas chromatography-mass spectrometry, J. Chromatogr. 228 (1982) 195–203, https://doi.org/10.1016/s0378-4347(00)80432-6.

[12] L. Laviana, I. Llorente, M. Bayod, D. Blanco, In-process control of midazolam synthesis by HPLC, J. Pharmaceut. Biomed. Anal. 32 (2003) 167–174, https://doi.org/10.1016/S0731-7085(03)00057-8.

[13] C.B. Eap, G. Bouchoux, K.P. Golay, P. Baumann, Determination of picogram levels of midazolam, and 1- and 4-hydroxymidazolam in human plasma by gas chromatography-negative chemical ionization-mass spectrometry, J. Chromatogr. B 802 (2004) 339–345, https://doi.org/10.1016/j.jchromb.2003.12.014.

[14] B. Narayana, K. Divya, Prankash S. Nayak, Selective and validated spectrophotometric methods for the determination of midazolam using N-bromosuccinimide, J. Chem. Pharmaceut. Res. 5 (2013) 268–274.

[15] B. Lausecker, G. Hopfgartner, M. Hesse, Capillary electrophoresis-mass spectrometry coupling versus micro-high-performance liquid chromatography-mass spectrometry coupling: a case study, J. Chromatogr. B Biomed. Appl. 718 (1998) 1–13, https://doi.org/10.1016/S0378-4347(98)00358-2.

[16] A. Chen, B. Shah, Electrochemical sensing and biosensing based on square wave voltammetry, Anal. Methods. 5 (2013) 2158–2173, https://doi.org/10.1039/c3ay40155c.

[17] J. Adkins, K. Boehle, C. Henry, Electrochemical paper-based microfluidic devices, Electrophoresis 36 (2015) 1811–1824, https://doi.org/10.1002/elps.201500084.

[18] V.N. Ataide, L.F. Mendes, L.I.L.M. Gama, W.R. De Araujo, T.R.L.C. Paixão, Electrochemical paper-based analytical devices: ten years of development, Anal. Methods. 12 (2020) 1030–1054, https://doi.org/10.1039/c9ay02350j.

[19] J.M. Oh, K.F. Chow, Recent developments in electrochemical paper-based analytical devices, Anal. Methods. 7 (2015) 7951–7960, https://doi.org/10.1039/c5ay01724f.

[20] E. Noviana, C.P. McCord, K.M. Clark, I. Jang, C.S. Henry, Electrochemical paper-based devices: sensing approaches and progress toward practical applications, Lab Chip 20 (2020) 9–34, https://doi.org/10.1039/c9lc00903e.

[21] W. Dungchai, O. Chailapakul, C.S. Henry, Electrochemical detection for paper-based microfluidics, Anal. Chem. 81 (2009) 5821–5826, https://doi.org/10.1021/ac9007573.

[22] T.R. de Oliveira, W.T. Fonseca, G.O. Setti, R.C. Faria, Fast and flexible strategy to produce electrochemical paper-based analytical devices using a craft cutter printer to create wax barrier and screen-printed electrodes, Talanta 195 (2019) 480–489, https://doi.org/10.1016/j.talanta.2018.11.047.

[23] C.L.S. Chagas, L.C. Duarte, E.O. Lobo-Júnior, E. Piccin, N. Dossi, W.K.T. Coltro, Hand drawing of pencil electrodes on paper platforms for contactless conductivity detection of inorganic cations in human tear samples using electrophoresis chips, Electrophoresis 36 (2015) 1837–1844, https://doi.org/10.1002/elps.201500110.

[24] L.O. Orzari, I.A.A. Andreotti, M.F. Bergamini, L.H.M. Junior, B.C. Janegitz, Disposable electrode obtained by pencil drawing on corrugated fiberboard substrate, Sensor. Actuator. B Chem. 264 (2018) 20–26, https://doi.org/10.1016/j.snb.2018.02.162.

[25] W.R. de Araujo, C.M.R. Frasson, W.A. Ameku, J.R. Silva, L. Angnes, T.R.L. C. Paixão, Single-step reagentless laser scribing fabrication of electrochemical paper-based analytical devices, Angew. Chem. 56 (2017) 15113–15117, https://doi.org/10.1002/ange.201708527.

[26] V.X.G. Oliveira, A.A. Dias, L.L. Carvalho, T.M.G. Cardoso, F. Colmati, W.K. T. Coltro, Determination of ascorbic acid in commercial tablets using pencil drawn electrochemical paper-based analytical devices, Anal. Sci. 34 (2018) 91–95, https://doi.org/10.2116/analsci.34.91.

[27] J.R. Camargo, I.A.A. Andreotti, C. Kalinke, J.M. Henrique, J.A. Bonacin, B. C. Janegitz, Waterproof paper as a new substrate to construct a disposable sensor for the electrochemical determination of paracetamol and melatonin, Talanta 208 (2020) 120458, https://doi.org/10.1016/j.talanta.2019.120458.

[28] B.B. Prasad, R. Singh, A new micro-contact imprinted L-cysteine sensor based on sol-gel decorated graphite/multiwalled carbon nanotubes/gold nanoparticles composite modified sandpaper electrode, Sensor. Actuator. B Chem. 212 (2015) 155–164, https://doi.org/10.1016/j.snb.2015.01.119.

[29] Y. Xu, L. Hou, H. Zhao, S. Bi, L. Zhu, Y. Lu, Alumina sandpaper-supported nickel nanocoatings and its excellent apllication in non-enzymatic glucose sensing, Appl. Surf. Sci. 463 (2019) 1028–1036, https://doi.org/10.1016/j.apsusc.2018.08.248.

[30] P.J. Lamas-Ardisana, P. Casuso, I. Fernandez-Gauna, G. Martínez-Paredes, E. Jubete, L. Añorga, G. Cabañero, H.J. Grande, Disposable electrochemical paper-based devices fully fabricated by screen-printing technique, Electrochem. Commun. 75 (2017) 25–28, https://doi.org/10.1016/j.elecom.2016.11.015.

[31] L.A. Pradela-Filho, I.A.A. Andreotti, J.H.S. Carvalho, D.A.G. Araújo, L.O. Orzari, A. Gatti, R.M. Takeuchi, A.L. Santos, B.C. Janegitz, Glass varnish-based carbon conductive ink: a new way to produce disposable electrochemical sensors, Sensor. Actuator. B Chem. 305 (2020) 127433, https://doi.org/10.1016/j.snb.2019.127433.

[32] C. Hu, X. Bai, Y. Wang, W. Jin, X. Zhang, S. Hu, Inkjet printing of nanoporous gold electrode arrays on cellulose membranes for high-sensitive paper-like electrochemical oxygen sensors using ionic liquid electrolytes, Anal. Chem. 84 (2012) 3745–3750, https://doi.org/10.1021/ac3003243.

[33] M. Reynolds, L.M. Duarte, W.K.T. Coltro, M.F. Silva, F.J.V. Gomez, C.D. Garcia, Laser-engraved ammonia sensor integrating a natural deep eutectic solvent, Microchem. J. 157 (2020) 105067, https://doi.org/10.1016/j.microc.2020.105067.

[34] A.A. Kava, C. Beardsley, J. Hofstetter, C.S. Henry, Disposable glassy carbon stencil printed electrodes for trace detection of cadmium and lead, Anal. Chim. Acta 1103 (2020) 58–66, https://doi.org/10.1016/j.aca.2019.12.047.

[35] N. Dossi, R. Toniolo, A. Pizzariello, F. Impellizzieri, E. Piccin, G. Bontempelli, Pencil-drawn paper supported electrodes as simple electrochemical detectors for paper-based fluidic devices, Electrophoresis 34 (2013) 2085–2091, https://doi.org/10.1002/elps.201200425.

[36] N. Dossi, F. Terzi, E. Piccin, R. Toniolo, G. Bontempelli, Rapid prototyping of sensors and conductive elements by day-to-day writing tools and emerging manufacturing technologies, Electroanalysis 28 (2016) 250–264, https://doi.org/10.1002/elan.201500361.

[37] W. Li, D. Qian, Q. Wang, Y. Li, N. Bao, H. Gu, C. Yu, Fully-drawn origami paper analytical device for electrochemical detection of glucose, Sensor. Actuator. B Chem. 231 (2016) 230–238, https://doi.org/10.1016/j.snb.2016.03.031.

[38] M. Santhiago, M. Strauss, M.P. Pereira, A.S. Chagas, C.C.B. Bufon, Direct drawing method of graphite onto paper for high-performance flexible electrochemical sensors, ACS Appl. Mater. Interfaces 9 (2017) 11959–11966, https://doi.org/10.1021/acsami.6b15646.

[39] Z. Li, F. Li, J. Hu, W.H. Wee, Y.L. Han, B. Pingguan-Murphy, T.J. Lu, F. Xu, Direct writing electrodes using a ball pen for paper-based point-of-care testing, Analyst 140 (2015) 5526–5535, https://doi.org/10.1039/c5an00620a.

[40] V.N. Ataide, W.A. Ameku, R.P. Bacil, L. Angnes, W.R. de Araujo, T.R.L. Paixão, Enhanced performance of pencil-drawn paper-based electrodes by laser-scribing treatment, RSC Adv. 11 (2021) 1644–1653. https://doi.org/10.1039/d0ra08874a.

[41] G. Scordo, D. Moscone, G. Palleschi, F. Arduini, A reagent-free paper-based sensor embedded in a 3D printing device for cholinesterase activity measurement in serum, Sensor. Actuator. B Chem. 258 (2018) 1015–1021, https://doi.org/10.1016/j.snb.2017.11.134.

[42] R.M. Cardoso, C. Kalinke, R.G. Rocha, P.L. dos Santos, D.P. Rocha, P.R. Oliveira, B. C. Janegitz, J.A. Bonacin, E.M. Richter, R.A.A. Munoz, Additive-manufactured (3D-printed) electrochemical sensors: a critical review, Anal. Chim. Acta 1118 (2020) 73–91, https://doi.org/10.1016/j.aca.2020.03.028.

[43] G. Li, X. Mo, W. Law, K.C. Chan, A wearable fluid capture device for electrochemical sensing of sweat, ACS Appl. Mater. Interfaces 11 (2019) 238–243, https://doi.org/10.1021/acsami.8b17419.

[44] L.C. Duarte, F. Figueredo, L.E.B. Ribeiro, E. Cortón, W.K.T. Coltro, Label-free counting of Escherichia coli cells in nanoliter droplets using 3D printed

microfluidic devices with integrated contactless conductivity detection, Anal. Chim. Acta 1071 (2019) 36–43, https://doi.org/10.1016/j.aca.2019.04.045.
[45] Z. Liu, Y. Zhang, S. Xu, H. Zhang, Y. Tan, C. Ma, R. Song, L. Jiang, C. Yi, A 3D printed smartphone optosensing platform for point-of-need food safety inspection, Anal. Chim. Acta 966 (2017) 81–89, https://doi.org/10.1016/j.aca.2017.02.022.
[46] N.C. de Moraes, E.N.T. da Silva, J.M. Petroni, V.S. Ferreira, B.G. Lucca, Design of novel, simple, and inexpensive 3D printing-based miniaturized electrochemical platform containing embedded disposable detector for analytical applications, Electrophoresis 41 (2020) 278–286, https://doi.org/10.1002/elps.201900270.
[47] L.A. Pradela-Filho, D.A.G. Araújo, R.M. Takeuchi, A.L. Santos, Nail polish and carbon powder: an attractive mixture to prepare paper-based electrodes, Electrochim. Acta 258 (2017) 786–792, https://doi.org/10.1016/j.electacta.2017.11.127.
[48] D. Martín-Yerga, I. Álvarez-Martos, M.C. Blanco-López, C.S. Henry, M. T. Fernández-Abedul, Point-of-need simultaneous electrochemical detection of lead and cadmium using low-cost stencil-printed transparency electrodes, Anal. Chim. Acta 981 (2017) 24–33, https://doi.org/10.1016/j.aca.2017.05.027.
[49] W.A. Ameku, W.R. de Araujo, C.J. Rangel, R.A. Ando, T.R.L.C. Paixão, Gold nanoparticle paper-based dual-detection device for forensics applications, ACS Appl. Nano Mater. 2 (2019) 5460–5468, https://doi.org/10.1021/acsanm.9b01057.
[50] E.Y. Jomma, N. Bao, S.N. Ding, A pencil drawn microelectrode on paper and its application in two-electrode electrochemical sensors, Anal. Methods 9 (2017) 3513–3518, https://doi.org/10.1039/c7ay00605e.
[51] M.A. Pimenta, G. Dresselhaus, M.S. Dresselhaus, L.G. Cançado, A. Jorio, R. Saito, Studying disorder in graphite-based systems by Raman spectroscopy, Phys. Chem. Chem. Phys. 9 (2007) 1276–1291, https://doi.org/10.1039/b613962k.
[52] A.A. Dias, C.L.S. Chagas, H.A. Silva-Neto, E.O. Lobo-Junior, L.F. Sgobbi, W.R. De Araujo, T.R.L.C. Paixão, W.K.T. Coltro, Environmentally friendly manufacturing of flexible graphite electrodes for a wearable device monitoring zinc in sweat, ACS Appl. Mater. Interfaces 11 (2019) 39484–39492, https://doi.org/10.1021/acsami.9b12797.
[53] T.A. Silva, H. Zanin, E. Saito, R.A. Medeiros, F.A. Vicentini, E.J. Corat, O. Fatibello-filho, Electrochemical behaviour of vertically aligned carbon nanotubes and graphene oxide nanocomposite as electrode material, Electrochim. Acta 119 (2014) 114–119, https://doi.org/10.1016/j.electacta.2013.12.024.
[54] N. Dossi, S. Petrazzi, F. Terzi, R. Toniolo, G. Bontempelli, Electroanalytical cells pencil drawn on PVC supports and their use for the detection in flexible microfluidic devices, Talanta 199 (2019) 14–20, https://doi.org/10.1016/j.talanta.2019.01.126.
[55] C.A. O'boyle, D. Harris, H. Barry, C. Mccreary, A. Bewley, E. Fox, Comparison of midazolam by mouth and diazepam I.V. in outpatient oral surgery, Br. J. Anaesth. 59 (1987) 746–754, https://doi.org/10.1093/bja/59.6.746.
[56] M.R. Ganjali, B. Larijani, P. Norouzi, Determination of midazolam by potentiometric PVC membrane and MWCNTs based carbon paste sensors, Int. J. Electrochem. Sci. 7 (2012) 4822–4833.
[57] N. Ghorbani, S. Hosseinzadeh, S. Pashaei, A. Hosseinzadeh, H.A. Hamidi, The effect of produce conditions for preparation of potentiometric carbon paste sensor for determination of midazolam in pharmaceutical, Int. J. Electrochem. Sci. 9 (2014) 3772–3783.
[58] J.C. Vire, G.J. Patriarche, B.G. Hermosa, Polarographic behaviour and hydrolysis of midazolam and its metabolites, Anal. Chim. Acta 196 (1987) 205–212, https://doi.org/10.1016/S0003-2670(00)83085-8.
[59] C.M. dos Santos, V. Famila, S.M. Gonçalves, Square-wave voltammetric techniques for determination of psychoactive 1,4-benzodiazepine drugs, Anal. Bioanal. Chem. 374 (2002) 1074–1081, https://doi.org/10.1007/s00216-002-1535-0.